Pten ablation in adult dopaminergic neurons is neuroprotective in Parkinson's disease models

Andrii Domanskyi,* Christin Geißler,* Ilya A. Vinnikov,* Heike Alter,* Andreas Schober,† Miriam A. Vogt,‡ Peter Gass,‡ Rosanna Parlato,* and Günther Schütz*,[1]

*Division of Molecular Biology of the Cell I, German Cancer Research Center, Heidelberg, Germany; †Department of Molecular Embryology, Institute for Anatomy and Cell Biology II, University of Freiburg, Freiburg, Germany; and ‡Central Institute of Mental Health, RG Animal Models in Psychiatry, University of Heidelberg, Mannheim, Germany

ABSTRACT **Parkinson's disease (PD) is a progressive age-related movement disorder that results primarily from the selective loss of midbrain dopaminergic (DA) neurons. Symptoms of PD can be induced by genetic mutations or by DA neuron-specific toxins. A specific ablation of an essential factor controlling ribosomal RNA transcription, TifIa, in adult mouse DA neurons represses mTOR signaling and leads to progressive neurodegeneration and PD-like phenotype. Using an inducible Cre system in adult mice, we show here that the specific ablation of Pten in adult mouse DA neurons leads to activation of mTOR pathway and is neuroprotective in genetic (*TifIa* deletion) and neurotoxin-induced (MPTP or 6OHDA) mouse models of PD. Adult mice with DA neuron-specific *Pten* deletion exhibit elevated expression of tyrosine hydroxylase, a rate-limiting enzyme in the dopamine biosynthesis pathway, associated with increased striatal dopamine content, and increased mRNA levels of *Foxa2*, *Pitx3*, *En1*, *Nurr1*, and *Lmx1b*—the essential factors for maintaining physiological functions of adult DA neurons. *Pten* deletion attenuates the loss of tyrosine hydroxylase-positive cells after 6OHDA treatment, restores striatal dopamine in *TifIa*-knockout and MPTP-treated mice, and rescues locomotor impairments caused by *TifIa* loss. Inhibition of Pten-dependent functions in adult DA neurons may represent a promising PD therapy.—Domanskyi, A., Geißler, C., Vinnikov, I. A., Alter, H., Schober, A., Vogt, M. A., Gass, P., Parlato, R., Schütz, G. *Pten* ablation in adult dopaminergic neurons is neuroprotective in Parkinson's disease models. *FASEB J.* 25, 2898–2910 (2011). www.fasebj.org**

Key Words: neurodegeneration · mTOR · mouse

Neurodegenerative diseases such as Alzheimer's disease, Huntington's disease, and Parkinson's disease (PD) are among the most devastating age-related disorders in humans. PD is a progressive movement disorder resulting primarily from the selective loss of dopaminergic (DA) neurons in the substantia nigra. The majority of PD cases are sporadic; however, ~3% of PD cases are associated with genomic mutations. The affected genes include α-synuclein, parkin, leucine-rich repeat kinase 2 (LRRK2), DJ-1, and phosphatase and tensin homologue deleted on chromosome 10 (PTEN)-induced kinase 1 (PINK1) (1). Symptoms of PD can also be induced by DA neuron-specific toxins, such as 6-hydroxydopamine (6OHDA), rotenone, and 1-methyl-4-phenyl-1,2,3,6 tetrahydropyridine (MPTP) (2, 3). Functional analysis of pathways affected by these genomic mutations and toxins implicated mitochondrial dysfunction and oxidative stress as important factors in the pathogenesis of PD (4). Recent data demonstrate a functional link between PINK1 and parkin in maintaining mitochondrial integrity. PINK1 accumulates on damaged mitochondria and recruits and directly phosphorylates parkin, leading to activation of its ubiquitin-protein ligase activity that promotes a selective autophagy of damaged mitochondria (5–7). Notably, PD-associated mutations in PINK1 and parkin disrupt this pathway (8). Several genetic animal models have been created to study the mechanisms behind PD development. However, most of these genetic mouse models fail to recapitulate all symptoms of human PD (9, 10).

We have previously demonstrated that a disruption of ribosomal RNA synthesis through the genetic ablation of *TifIa*, an essential factor controlling RNA polymerase I (Pol I)-mediated transcription, leads to progressive neurodegeneration (11). Using transgenic mice with DA neuron-specific expression of inducible Cre recombinase, we have achieved a specific and temporally controlled ablation of *TifIa* in adult DA neurons. Compared to the neurotoxin-induced models of PD, such an inducible genetic system offers higher specificity and selectivity toward DA neuronal population. The mice lacking TifIa selectively in adult neurons exhibit a

[1] Correspondence: Molecular Biology of the Cell I, German Cancer Research Center, Im Neuenheimer Feld 280, D-69120 Heidelberg, Germany. E-mail: g.schuetz@dkfz.de

doi: 10.1096/fj.11-181958

This article includes supplemental data. Please visit *http://www.fasebj.org* to obtain this information.

0892-6638/11/0025-2898 © FASEB

PD-like phenotype and, therefore, represent a novel animal model recapitulating essential hallmarks of PD development and progression. Notably, TifIa loss in DA neurons results in nucleolar disruption and down-regulation of Akt/mTOR signaling (12).

A lipid phosphatase Pten antagonizes the Akt/mTOR signaling pathway regulating cell growth and survival, as well as apoptosis and autophagy (13). Pten can interact with components of the Pol I transcription complex and down-regulate ribosomal RNA synthesis (14). Because of its inhibitory effects on the Akt/mTOR prosurvival pathway, Pten may play a role in PD development (15). PD-related protein DJ-1 suppresses Pten function in *Drosophila* and in cultured cells (16). Down-regulation of Pten in neurotoxin-treated cells reduces intracellular levels of reactive oxygen species (17). Brain-specific *Pten* deletion during early embryonic development causes defects in neuronal migration, increased neuronal soma and nucleoli size, altered branching morphology, seizures, and ataxia that are probably due to defects in synaptic transmission and myelination abnormalities (18–21). In contrast, *Pten* ablation in developing DA neurons is protective against acute neurotoxic insult (22). However, since in these models *Pten* expression in the brain is ablated already during neuronal differentiation, these results may not fully reflect the functions of this protein in adult neurons. Moreover, while all previous publications show that Pten loss protects neurons against acute neurotoxic stress *in vitro* and *in vivo* (17, 22), the neuroprotective potential of Pten ablation in genetic model of PD has never been observed up to now.

Here, we demonstrate a neuroprotective role of *Pten* ablation in a genetic progressive model of PD caused by the loss of *TifIa* and in neurotoxin-induced PD models. In *TifIa/Pten*-knockout mice, *Pten* loss partially restored striatal dopamine and completely rescued locomotor deficits associated with *TifIa* ablation. We further show that specific *Pten* deletion in adult DA neurons protected these neurons from 6OHDA toxicity and restored striatal dopamine in MPTP-treated mice. Notably, *Pten* ablation in adult DA neurons did not result in any obvious phenotypic abnormalities. These results indicate that inhibiting Pten-dependent functions in adult DA neurons has a neuroprotective effect that can be used for therapeutic interventions.

MATERIALS AND METHODS

Experimental mice and tamoxifen (Tam) treatment

Mice were maintained in C57BL/6 genetic background on a 12-h light-dark cycle with free access to water and food. The $Pten^{fl/fl}$/DATCreERT2 mouse line was generated by mating $Pten^{fl/fl}$ mice (23) with DATCreERT2 mice (24). To generate $TifIa^{fl/fl}$/$Pten^{fl/fl}$/DATCreERT2 mice, $Pten^{fl/fl}$/DATCreERT2 animals were mated with $TifIa^{fl/fl}$ mice (25). Inducible Cre recombinase was activated in 8- to 10-wk-old mice by intraperitonial injections of 1 mg Tam (Sigma, St. Louis, MO, USA) diluted in sunflower oil 2×/d for 5 d (see **Fig. 1*A***). Littermates harboring only floxed alleles were used as controls. All experimental procedures were approved by the Committee of Animal Care and Use (Regierungspräsidium Karlsruhe) and carried out in accordance with EU guidelines on animal care.

Immunohistochemistry and immunoblotting

Mice were perfused with 4% PFA; the brains were dissected and were fixed overnight in 4% PFA and processed for either paraffin or vibratome sections. Immunohistochemical staining was performed as described previously (11), using the following antibodies: anti-tyrosine hydroxylase (TH; 1:1000, AB1542; Millipore, Billerica, MA, USA), anti-nucleophosmin (NPM; 1:1000, MAB4500; Millipore), anti-phospho-Akt (pAkt; 1:50, 4058; Cell Signaling, Beverly, MA, USA), anti-phospho-S6 (pS6; 1:50, 4857; Cell Signaling), anti-Pten (1:50, 9559; Cell Signaling), anti-dopamine transporter (DAT; 1:500, MAB369; Millipore).

For the preparation of total protein extracts and RNA isolation, the mice were sacrificed by asphyxiation with CO_2, the brains were dissected, and 2-mm striatal or ventral midbrain slices were cut using a 1-mm brain matrix (Alto, Leominster, MA, USA). Total RNA and protein extraction was performed with AllPrep DNA/RNA/Protein Mini Kit (Qiagen, Venlo, The Netherlands) according to manufacturer's instructions. Total protein extracts (50 μg) from ventral midbrain or striatum were used for immunoblotting with anti-TH (1:5000), anti-Pten (1:2000), anti-Akt (1:2000, 4685; Cell Signaling), anti-S6 (1:2000, 2217; Cell Signaling), anti-pAkt (1:1000), and anti-pS6 (1:500), or anti-PINK1 (1:500, 10006283; Cayman Chemicals) antibody and with anti-GAPDH (1:10000, MAB374; Millipore) as a loading control. Images were acquired with the LAS-3000 imaging system (Fuji, Tokyo, Japan); band intensity was quantified using ImageGauge software (Fuji) and normalized to that of control samples.

Quantitative analyses of DA neurons and striatal TH immunoreactivity

Neuronal numbers and morphology were quantified on micrographs from stained brain sections using MCID Image Analysis software (InterFocus Imaging, UK). The number of TH^+ or Nissl-stained neurons in substantia nigra, identified according to the anatomical landmarks (26), was quantified on coronal paraffin sections (7 μm), immunostained with anti-TH antibody, or stained with cresyl violet. The values were calculated for each mouse from ≥12 sections covering rostral substantia nigra. To quantify the nucleolar disruption levels in TH^+ neurons of *TifIa* and *TifIa/Pten* double-knockout mice, similar analysis was performed on paraffin sections immunostained with anti-TH and anti-NPM antibodies. Nucleoli diameter and cell area of TH^+ neurons on the midbrain sections immunostained with anti-TH/anti-NPM antibodies, as well as the optical density of DAT- or TH-immunostained striatal sections were quantified using ImageJ software (http://rsbweb.nih.gov/ij/). Image analysis and neuronal counts were performed independently by more than one investigator, masked to the experimental conditions.

Quantitative RT-PCR

Total RNA isolated from striatal and ventral midbrain samples of control and mutant mice served as a template for DNA synthesis using Super-Script III first-strand synthesis kit (Invitrogen). For genomic DNA contamination control, samples

with no added reverse transcriptase enzyme were included. Quantitative PCR was performed with a Chromo4 real-time PCR detection system (Bio-Rad, Hercules, CA, USA) using TaqMan gene expression assays (Applied Biosystems, Foster City, CA, USA), according to the manufacturer's instructions. The mRNA levels of *TH, En1, Pitx3, Nurr1, Lmx1b, Foxa1*, and *Foxa2* in the samples from the mutant mice were normalized to those of controls. The mRNA levels of two housekeeping genes, *Hprt1* and *B2m*, were measured to control for the equal amount of input cDNA.

Striatal dopamine content measurements

Striatal dopamine content measurements were performed by the HPLC-electrochemical detection method (HPLC-ED), as described previously (27).

MPTP and 6OHDA treatments

The mice were intraperitoneally injected 1×/d with 20 mg/kg body weight 1-methyl-4-phenyl-1,2,3,6 tetrahydropyridine hydrochloride (MPTP; Sigma, St. Louis, MO, USA) for 3 d (28) and sacrificed 5 d after the last injection.

For the unilateral stereotactic intrastriatal 6OHDA injections, control and *Pten*-knockout mice 19 wk after the onset of *Pten* deletion were anesthetized with ketamine/xylazine and placed in a stereotactic frame (David Kopf Instruments, Tujunga, CA, USA). 6OHDA (Sigma) was diluted in 0.9% NaCl to 5.0 mg/ml final concentration, and a total dose of 15.0 μg (3 μl) was injected using a glass capillary into the striatum at AP: +0.4 mm; ML: +1.8 mm; DV: −3.5 mm relative to bregma. Sham-operated mice received 3 μl 0.9% NaCl intrastriatal injection to the same coordinates. The capillary was slowly withdrawn after 3–5 min. The animals were sacrificed for analysis 10 d after the injection (see **Fig. 4*B***). Sham-operated mice did not show any changes in TH^+ neuronal numbers and in striatal dopamine content (data not shown).

Behavioral assays

The constant-speed rotarod assay to measure forelimb and hindlimb motor coordination and balance was performed using the rotarod apparatus (Ugo Basile, Biological Research Apparatus, Varese, Italy). During the training period, each mouse was placed on the rotarod at a constant speed (15 rpm) for several trials per day until all of the mice attained a stable baseline level of performance, staying at the 15 rpm

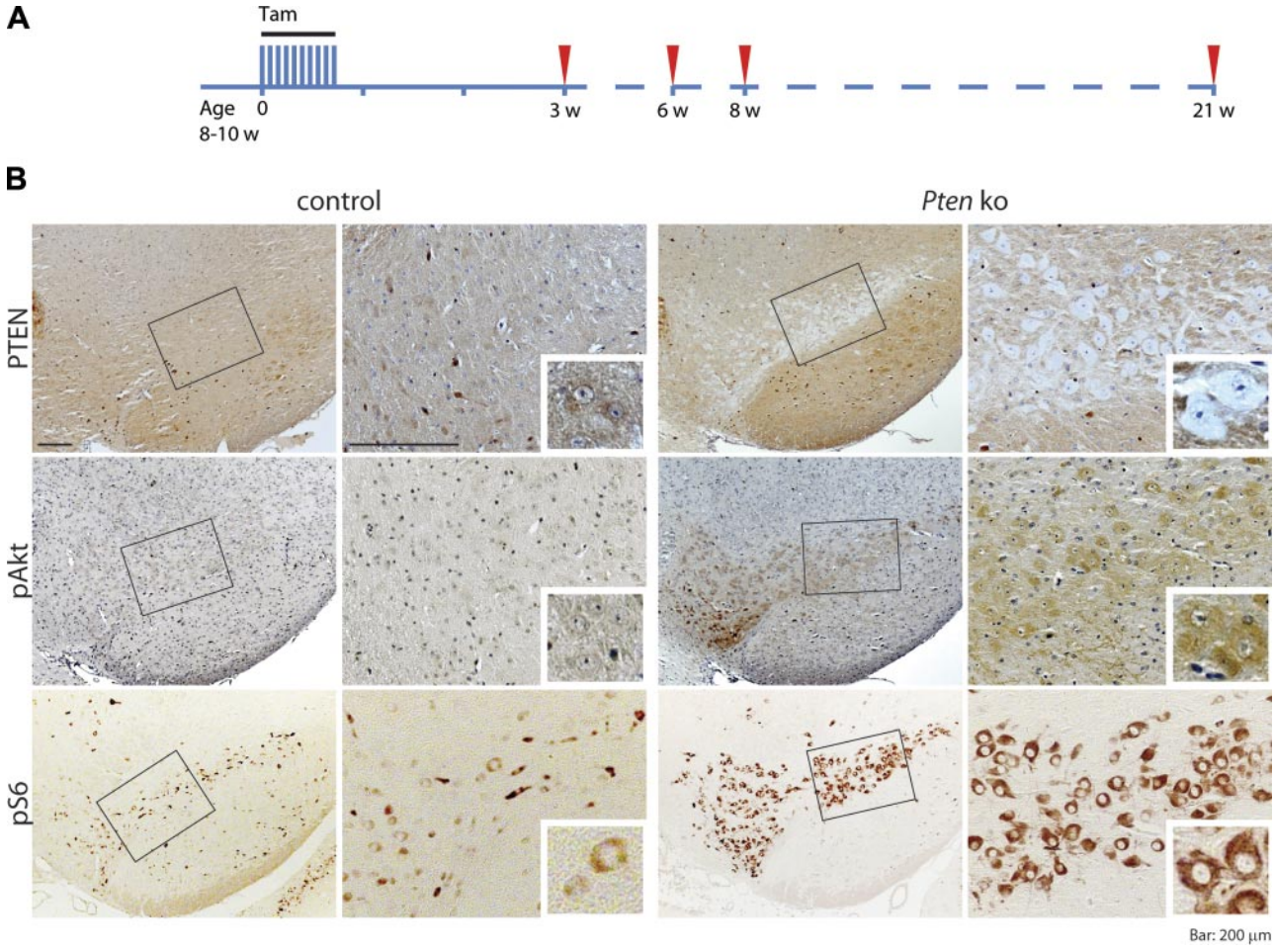

Figure 1. *Pten* ablation leads to Akt/mTOR pathway activation in adult DA neurons. *A*) Experimental timeline. *Pten* deletion was induced by Tam injections in 8- to 10-wk-old mice. At the indicated time points (red arrowheads), the mice were sacrificed, and the brains were dissected and processed for immunostaining, HPLC, or RNA/protein extraction as described in Materials and Methods. *B*) Loss of *Pten* and increase in phosphorylation of Akt and ribosomal protein S6 in *Pten*-knockout (*Pten* ko) animals 3 wk after the first Tam injection, visualized by immunostaining using specific antibodies. Insets: higher magnifications of representative neurons. Scale bar: 200 μm.

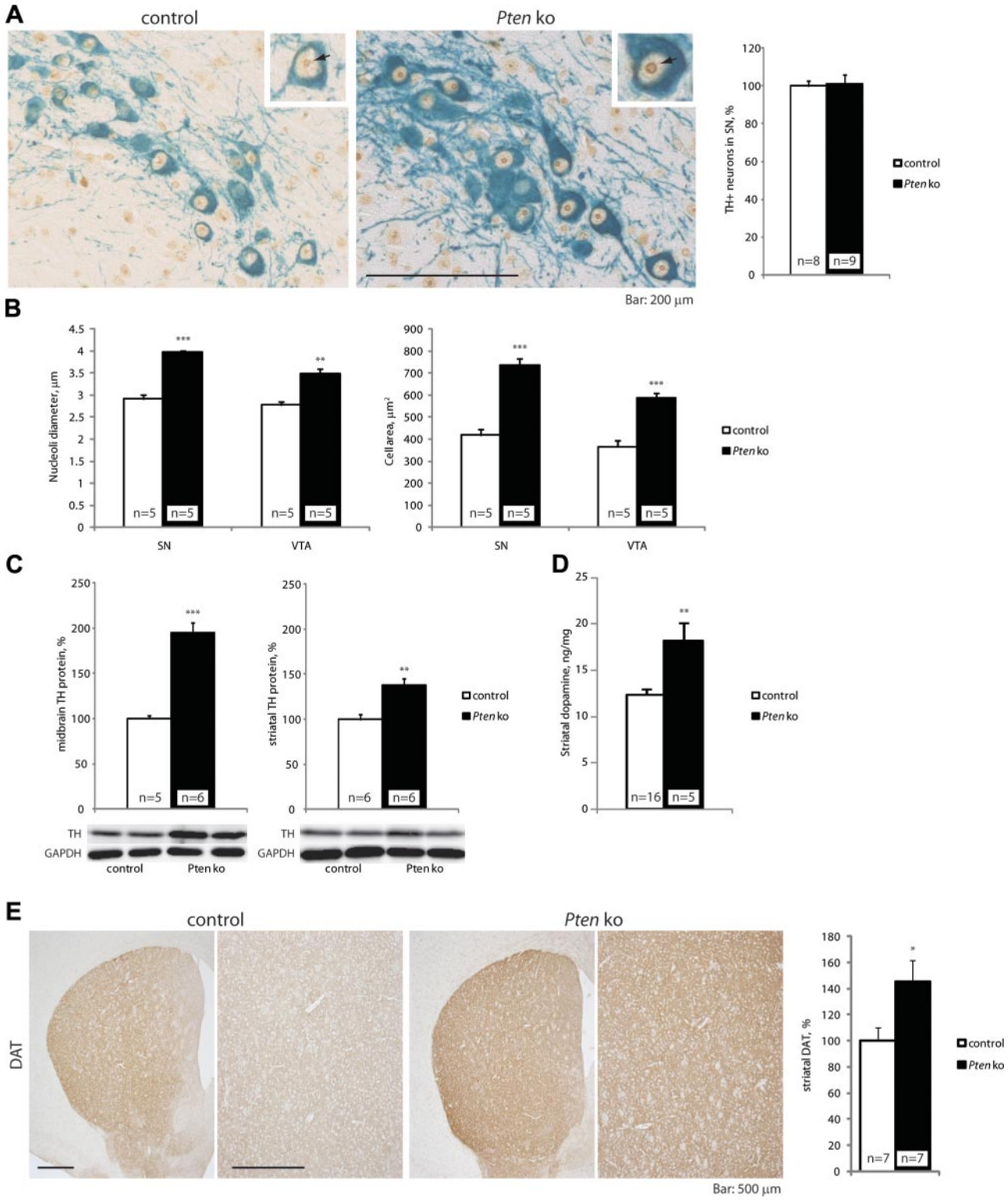

Figure 2. Increased neuronal soma and nucleolar size, TH protein expression, and striatal dopamine content in *Pten*-knockout mice. *A*) Increase in soma and nucleoli size in midbrain DA neurons, visualized by TH (blue) and NPM (brown) immunostaining, and quantification of TH^+ cell numbers in control and *Pten*-knockout mice 6 wk after the first Tam injection. Insets: higher magnifications of representative TH^+ neurons with NPM-immunostained nucleoli (arrows). *B*) Quantification of nucleolar diameter and cell area of TH^+ neurons in the substantia nigra (SN) and ventral tegmental area (VTA) in control and *Pten*-knockout mice 6 wk after the first Tam injection. *C*) Increase in TH protein levels was analyzed by quantitative immunoblotting of midbrain and striatal protein samples from control and *Pten*-knockout mice 8 wk after the first Tam injection. Equal loading of samples was controlled by immunoblotting with anti-GAPDH antibody. *D*) Striatal dopamine content increase in *Pten*-knockout mice, measured by HPLC 8 wk after the first Tam injection. *E*) Increase in the striatal density of DAT^+ axonal terminals in *Pten*-knockout mice, visualized by DAT immunostaining 6 wk after the first Tam injection. Scale bars = 200 μm (*A*); 500 μm (*E*). All data are expressed as means ± SE. $^*P < 0.05$, $^{**}P < 0.01$, $^{***}P < 0.001$ *vs.* control mice; Student's unpaired *t* test.

rotating rod for 60 s. Mice then received several trials at 15, 25, 35, and 44 rpm rotation speed with 60-s maximum trial length and 5-min intervals between individual trials, as described by Carter *et al.* (29). The mean latency to fall off the rotarod (for the two trials at each speed level) was recorded and used in subsequent analyses.

The footprint analysis was performed as described by Carter *et al.* (30). Briefly, the mice were trained to run toward an enclosed goal box in an open-top runway. The forepaws and hindpaws were painted with nontoxic paints of contrasting colors, and the mice were immediately placed on one end of the sheet of paper opposite the goal box. After drying, the footprint patterns were scanned and analyzed. For every mouse and for every step, the overlap between forepaw and hindpaw placement was defined as the average distance between the front and hind footprints on each side. For example, in **Fig. 5*A*,** the measured distances are shown as red (a_1, a_2,…, a_n) and blue (b_1, b_2,…, b_n) lines; the left overlap is the average length of lines a_1, a_2,…, a_n, and the right overlap is the average length of lines b_1, b_2,…, b_n. The overlap asymmetry was calculated as an absolute value of a difference between left and right overlaps (ref. 30; see Fig. 5*A*).

For the open field test, the mice were placed in a 50- × 50-cm arena illuminated with 25 lux from above for 10 min during their active period. Mice were placed individually into the arena and monitored for 10 min by a video camera (Sony CCD IRIS; Sony, Tokyo, Japan). The resulting data were analyzed using the image processing system EthoVision 3.0 (Noldus Information Technology, Wageningen, The Netherlands). For each sample, the system recorded position, object area, and the status of defined events. Parameters assessed were total traveled distance and average velocity. To measure grip strength, mice were held at the tail and lowered until they could hold with their forepaws the front bar of a triangle fixed at the grip strength apparatus (Bioseb, Chaville, France). After a few seconds, animals were pulled horizontally until they lost their grip. This was repeated 5 times, and the mean grip strength was calculated. The apparatus displayed the power of the grip in grams. For the wire hang test, the mice were put on a wire grid placed 60 cm above a cage filled with bedding. After 10 s, the grid was gently rotated to 90° within 1 s and held for 15 s. Then, the grid was rotated to 135° within 1 s and held for 15 s. The grid was rotated again to 180° and held for 20 s. The latency to fall off the grid and the angle of the wire grid were measured.

Statistical analyses

Statistical significance was calculated either by Student's 2-tailed unpaired *t* test or 2-way ANOVA followed by Bonferroni *post hoc* analyses for multiple comparisons, using GraphPad Prism software (GraphPad Scientific, San Diego, CA, USA). Data in text and figures are represented as means ± SE.

RESULTS

Pten deletion leads to Akt/mTOR pathway activation and increases in TH expression and striatal dopamine content

To exclude possible effects of *Pten* deletion on differentiation and activity of DA neurons during embryonic development, we specifically ablated *Pten* in adult mouse DA neurons using the Tam-inducible CreERT2/loxP system (31), where the expression of Cre recombinase fused to a modified ligand-binding domain of the estrogen receptor (CreERT2) is controlled by the regulatory elements of the DAT gene. In this study, we used DATCreERT2 mice in which the CreERT2 construct based on a bacterial artificial chromosome (BAC) harboring the DAT gene was integrated into the genome by insertion transgenesis (11, 24). Because of its large size, a BAC-based construct usually contains most of the regulatory elements necessary for the specific expression of CreERT2 independently of the genomic integration site (32), while not compromising the expression of endogenous DAT gene.

To induce *Pten* deletion in adult DA neurons, 8- to 10-wk-old *Pten*-knockout mice were injected with Tam and analyzed at different time points (3, 6, 8, and 21 wk) after induction of the mutation by Tam injections (**Fig. 1*A***).

The loss of Pten protein specifically in midbrain DA neurons, but not in the surrounding tissue containing other neuronal types and glial cells, was detectable by immunostaining 3 wk after Tam (Fig. 1*B*). *Pten* deletion resulted in increased levels of phosphorylated Akt, leading to the activation of Akt/mTOR pathway, as judged by the increase in phosphorylation of S6 protein, one of the downstream targets of mTOR (Fig. 1*B*). A significant increase in Akt and S6 phosphorylation was also evident in the immunoblot analysis of total protein extracts from the ventral midbrain of *Pten*-knockout and control mice (Supplemental Fig. S1). *Pten*-knockout mice exhibited reduced levels of Pten (Supplemental Fig. S1), with the remaining Pten protein signal most probably attributed to the other neuronal types and glial cells inevitably present in the dissected ventral midbrain samples.

Pten can induce the expression of a PD-associated protein, PINK1 (33); therefore, deletion of Pten may lead to PINK1 down-regulation. However, in our immunoblot analysis, the down-regulation of PINK1 protein in the ventral midbrain of *Pten*-knockout mice was not statistically significant (Supplemental Fig. S1). Notably, *Pten* ablation in adult DA neurons did not lead to changes in TH^+ cell numbers in the substantia nigra (**Fig. 2*A***). However, the cell bodies of DA neurons both

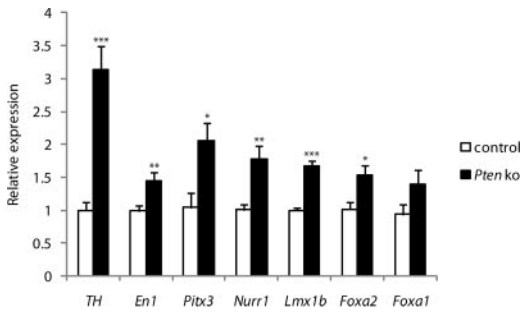

Figure 3. Increase in mRNA levels of midbrain DA neuron-specific genes in *Pten*-knockout mice. Quantification of the relative mRNA expression by qRT-PCR in dissected midbrain samples from control (n=7) and *Pten*-knockout mice (n=7) 8 wk after the first Tam injection. Data are expressed as means ± SE. *$P < 0.05$, **$P < 0.01$, ***$P < 0.001$ *vs.* control mice; Student's unpaired *t* test.

in the substantia nigra and in the ventral tegmental area (VTA) were significantly larger, with higher intensity of TH immunostaining in *Pten*-knockout mice as compared to control mice. The nucleoli of midbrain DA neurons visualized by immunostaining for the nucleolar protein NPM were also significantly enlarged (Fig. 2*A*, *B*). We also observed more pronounced TH immunostaining of neurofilaments in the substantia nigra reticulata in *Pten*-knockout mice (Figs. 2*A*, 6*A* and Supplemental Fig. S2*A*). Quantitative analysis of immunostained sections revealed a significant increase in the length and density of TH^+ neuronal fibers in *Pten*-knockout mice (Supplemental Fig. S2*A*).

To quantify the TH protein expression levels, we dissected the ventral midbrain region and the striatum and performed immunoblot analysis of total protein extracts from *Pten*-knockout and control mice 6 wk after beginning of Tam treatment. In agreement with the immunostaining results, we detected a significant upregulation of TH protein (Fig. 2*C*) and mRNA (**Fig. 3**) expression both in the ventral midbrain and in the striatum of *Pten*-knockout mice. *Pten*-knockout mice had increased striatal dopamine content (Fig. 2*D*) and striatal density of DAT^+ as well as TH^+ axonal terminals (Figs. 2*E* and Supplemental S2*B*).

Thus, *Pten* ablation in adult DA neurons led to Akt/mTOR pathway activation, significant enlargement of cell soma and nucleoli, higher TH expression in the midbrain DA neurons, and higher density of TH^+ axonal terminals in the striatum. Notably, increased TH levels in *Pten*-knockout mice were accompanied by significantly increased striatal dopamine content.

Pten-knockout mice have increased expression of specific genes involved in the maintenance of adult DA neurons

To elucidate the molecular mechanisms responsible for the observed cellular phenotype in *Pten*-knockout animals, we performed a quantitative RT-PCR analysis on the dissected ventral midbrain samples to quantify mRNA levels of several genes important for the development and also for the maintenance of DA neuronal population (34–37). Besides the increase in *TH*, adult *Pten*-knockout mice had significantly increased levels of *En1, Pitx3, Nurr1, Lmx1b*, and *Foxa2* mRNA in DA neurons, whereas the increase in *Foxa1* mRNA levels did not reach statistical significance (Fig. 3). *Foxa2*, *Pitx3*, and *Nurr1* are directly involved in regulation of *TH* expression during DA neuron development (37). Our results suggest that the elevated levels of these transcription factors may also promote TH expression in adult DA neurons, leading to elevated striatal dopamine content in *Pten*-knockout mice.

Pten-knockout mice are protected against MPTP and 6OHDA toxicity

To study the neuroprotective effect of *Pten* deletion in a neurotoxin-induced PD model, control and *Pten*-knockout mice were treated with MPTP. While the MPTP treatment led to a significant decrease in striatal dopamine content in controls, the levels of striatal dopamine remained elevated in MPTP-treated *Pten*-knockout mice (Fig. 4*A*).

The neuroprotective effect of *Pten* deletion was also evident in mice treated with a dopaminergic neuron-specific neurotoxin, 6OHDA (Fig. 4*B*). After a unilateral intrastriatal 6OHDA injection, the survival of nigral TH^+ neurons in control mice was 30% at the injected compared to the contralateral side, whereas in *Pten*-knockout mice, 51% of cells survived 6OHDA treatment (Fig. 4*C*, *D*). A similar result was obtained by performing total neuronal counts on Nissl-stained sections, confirming that the observed neuroprotective effect was indeed due to the increased cell survival after *Pten* deletion (Fig. 4*D*). Correspondingly, while in control mice striatal dopamine concentration at the injected site dropped to 1.7 ± 0.8 ng/mg, *Pten*-knockout animals retained 5.5 ± 0.7 ng/mg striatal dopamine at the injected side (Fig. 4*E*).

On a behavioral level, the footprint analysis revealed an asymmetry in overlap between forepaw and hindpaw placement in control mice after MPTP treatment (Fig. 5), whereas MPTP-treated *Pten*-knockout mice were not affected (Fig. 5*B*). Similar asymmetry was detected in *TifIa*-knockout, but not *TifIa/Pten* double-knockout mice (Fig. 5*B*). The overlap between forepaw and hindpaw placement is used to measure the accuracy of foot positioning and the uniformity of step alternation (30, 38), and the overlap asymmetry was the first early detectable behavioral abnormality in our experiments. Even though the overlap asymmetry may not reflect a specific loss of dopaminergic function, the asymmetric posture and gait have previously been reported in mice exhibiting DA neuron degeneration (39) and in patients with PD (40–42).

The deletion of *Pten* resulted in a significant increase in total striatal dopamine content not only in basal conditions but also after MPTP treatment. Moreover, *Pten* ablation was sufficient to attenuate the loss of TH^+ neurons and striatal dopamine in 6OHDA-treated mice, demonstrating that the loss of *Pten* is beneficial for the functional maintenance of adult DA neurons in stressed conditions.

Pten deletion attenuates the decline in striatal dopamine content and rescues locomotor deficits in a genetic model of PD

To assess whether *Pten* deletion has a neuroprotective role in a genetic progressive model of PD, we used our recently developed *TifIa*-knockout PD model and generated *TifIa/Pten* double-knockout mice to achieve the inducible tissue-specific deletion of both *TifIa* and *Pten* genes in adult DA neurons. At 8 wk after *TifIa* deletion, we observed a significant reduction in the number of TH^+ neurons in the substantia nigra of *TifIa* single-knockout mice (**Fig. 6*A*, *B***). Most of the remaining TH^+ neurons exhibited disrupted nucleoli and reduced

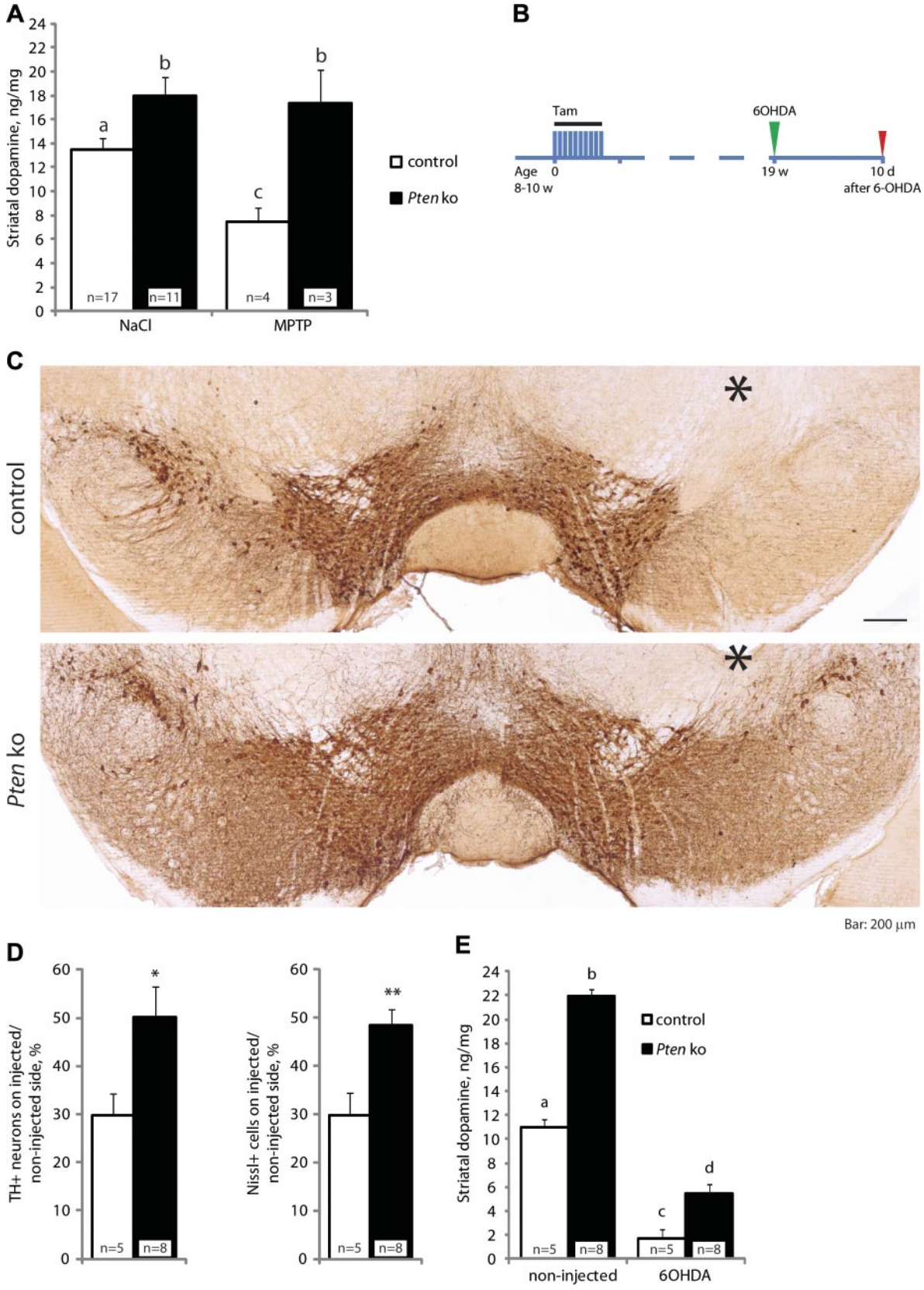

Figure 4. *Pten* deletion attenuates MPTP and 6OHDA toxicity. *A*) *Pten* ablation protects striatal dopamine levels, measured by HPLC, in *Pten*-knockout mice after MPTP treatment. Two-way ANOVA showed a significant effect of genotype (control *vs.* *Pten* ko, $P<0.0001$), and treatment × genotype interaction ($P=0.0356$). Groups with different superscript letters are statistically different ($P<0.05$; Bonferroni *post hoc* test). *B*) Timeline of the 6OHDA treatment experiments. *Pten* deletion was induced by Tam injections in 8- to 10-wk-old mice; 19 wk after the first Tam injection, mice received a unilateral stereotactic intrastriatal

(*continued on next page*)

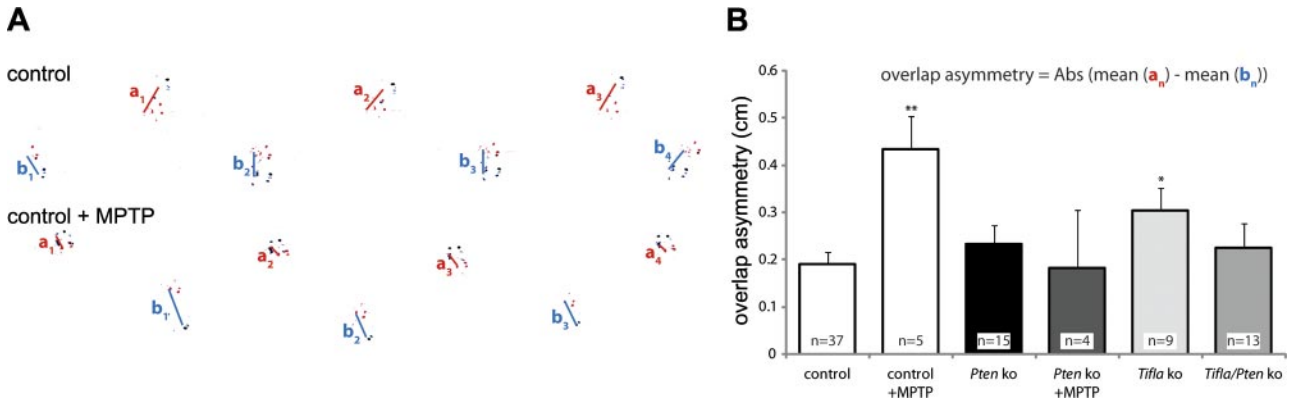

Figure 5. Pten deletion rescues gait abnormality caused by MPTP treatment or *TifIa* ablation. *A*) Representative footprint patterns from NaCl- and MPTP-treated control mice obtained in footprint analysis experiment. Overlap between forepaw and hindpaw placement was measured as mean distance between front and hind footprints on each side (means of a_1, a_2, a_3,…, a_n for left overlap and b_1, b_2, b_3,…, b_n for right overlap). Overlap asymmetry was calculated as an absolute value of a difference between left and right overlaps. Note that length of red and blue lines is similar for control mice, but is different for MPTP-treated mice. *B*) Asymmetry in overlap between forepaw and hindpaw placement in control and *Pten*-knockout mice treated with MPTP, and *TifIa* single-knockout and *TifIa/Pten* double-knockout mice. Data are expressed as means ± SE. $*P < 0.05$, $**P < 0.01$ *vs.* control mice; Student's unpaired *t* test.

soma size (Fig. 6*A*). *Pten* deletion could not prevent nucleolar disruption and degeneration of TH^+ nigral neurons, as similar levels of TH^+ neuronal loss and nucleolar disruption were also observed in *TifIa/Pten* double-knockout mice (Fig. 6*A*, *B*).

TifIa single-knockout mice developed a progressive decline of the striatal dopamine. While the average striatal dopamine concentration in control mice throughout the study period was 12.3 ± 0.5 ng/mg, in *TifIa* single-knockout mice, it was progressively reduced from 5.8 ± 0.4 ng/mg at 6 wk to 0.66 ± 0.03 ng/mg at 21 wk after beginning Tam treatment (Fig. 6*C*). In comparison to *TifIa*-knockout animals, the striatal dopamine level was significantly higher in *TifIa/Pten* double-knockout mice (Fig. 6*C*).

To attest whether the observed molecular phenotypes were accompanied by behavioral changes in the mutant mice, we performed several behavioral tests in control, *TifIa* or *Pten* single-knockout, and *TifIa/Pten* double-knockout mice. At 8 wk after the first Tam injection, control and knockout mice did not show statistically significant differences in distance and average speed in open field test, in grip strength, and in wire hang tests (data not shown). To assess the locomotor behavior of *TifIa* or *Pten* single-knockout and *TifIa/Pten* double-knockout mice, we utilized a constant speed rotarod assay that was shown to be highly sensitive in detecting locomotor deficits associated with early neurodegeneration stages (38, 43). At 6 wk after the beginning of Tam treatment, all tested mice were able to maintain the balance on the rotarod for 40–60 s at all rotation speeds (Fig. 6*D*). Control, *Pten* single-knockout, and *TifIa/Pten* double-knockout mice kept this ability until 21 wk after Tam. In contrast, beyond 10 wk after Tam treatment, *TifIa*-knockout mice exhibited a progressive decline in performance on the rotarod at all rotation speeds (Fig. 6*D*). At 10 wk after Tam treatment, *TifIa*-knockout mice did not maintain balance on the rotarod at the highest rotation speed (Fig. 6*D*, 44 rpm), and they performed significantly worse than *TifIa/Pten* double-knockout mice at 35 and 44 rpm (Fig. 6*D*, 35 rpm). By 21 wk after Tam, *TifIa*-knockout mice failed to maintain balance on the rotarod at higher rotation speeds for >5 s, and even at the lowest rotation speed, these mice could not perform for >15 s (Fig. 6*D*). *TifIa/Pten* double-knockout mice had no apparent problems with the balance at all rotation speeds and at all tested time points (Fig. 6*D*), indicating that *Pten* ablation rescued the progression of locomotor deficits caused by *TifIa* deletion in these mice.

DISCUSSION

The role of Akt/mTOR pathway and, particularly, Pten in the progression of cancer and PD is a subject of

injection of 15 μg 6OHDA and were sacrificed 10 d later, as described in Materials and Methods. *C*) DA neurons visualized by TH immunostaining on midbrain section from 6OHDA-injected control and *Pten*-knockout mice. Asterisk indicates injected side. Scale bar = 200 μm. *D*) Quantification of TH^+ and $Nissl^+$ cell numbers in the substantia nigra at the injected side in control and *Pten*-knockout mice 10 d after 6OHDA injection, relative to the corresponding number of cells at the side contralateral to the injection. $*P < 0.05$, $**P < 0.01$; Student's unpaired *t* test. *E*) *Pten* deletion attenuates the decline in striatal dopamine on 6OHDA-injected side of striatum, as measured by HPLC, in control and *Pten*-knockout mice. Two-way ANOVA showed a significant effect of treatment (6OHDA *vs.* noninjected, $P<0.0001$), genotype (control *vs. Pten* ko, $P<0.0001$), and treatment × genotype interaction ($P=0.0001$). Groups with different superscript letters are statistically different ($P<0.001$; Bonferroni *post hoc* test). All data are expressed as means ± SE.

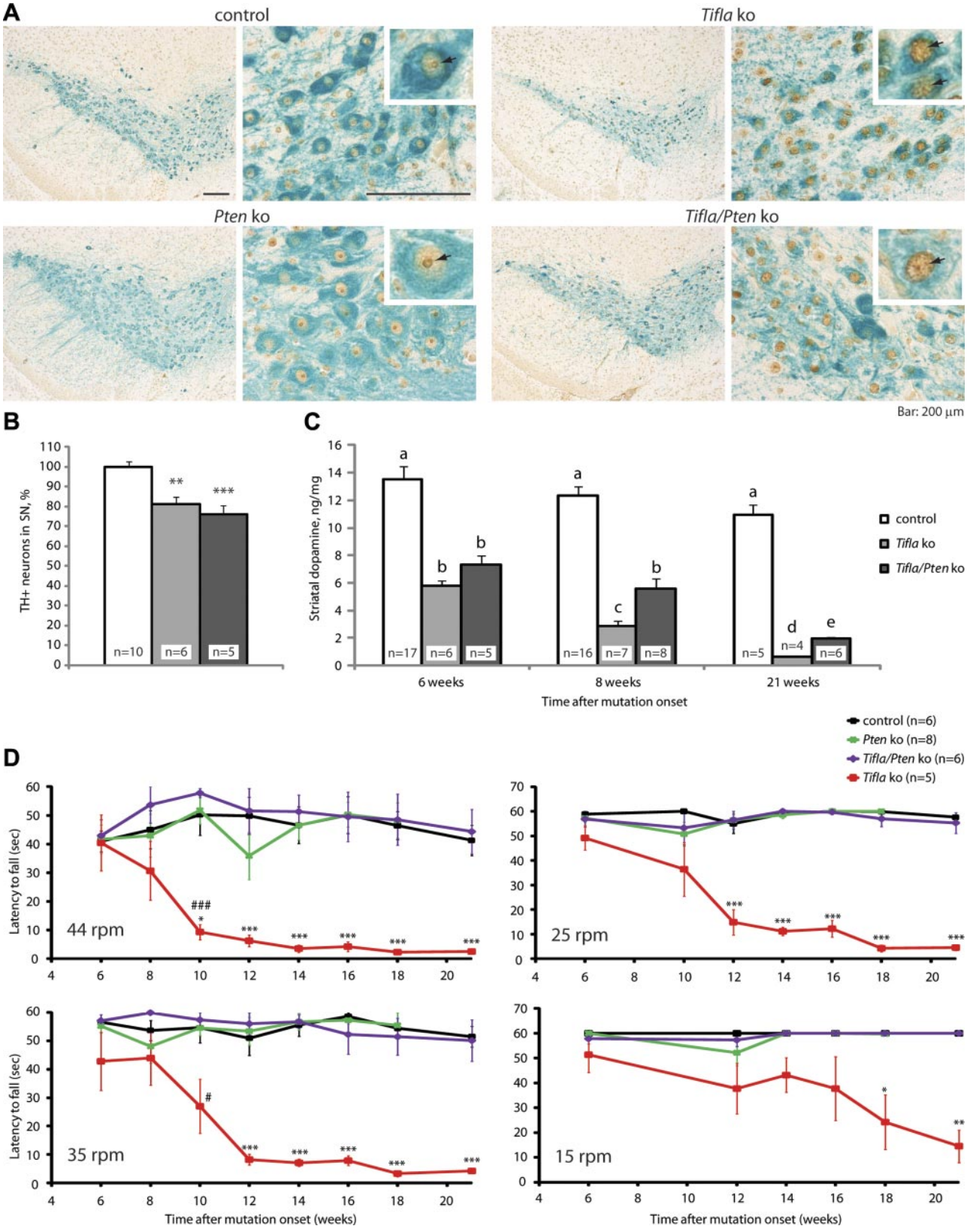

Figure 6. *Pten* deletion attenuates striatal dopamine decline and rescues locomotor deficits in *TifIa*-knockout model of PD. *A*) Increase in soma and nucleoli size in *Pten*-knockout mice and nucleoli disruption in *TifIa* single-knockout and *TifIa/Pten* double-knockout mice in the midbrain DA neurons, visualized by TH (blue) and NPM (brown) immunostaining. Insets: higher magnifications of representative TH^+ neurons with NPM-immunostained nucleoli in control and *Pten* single-knockout mice, and disrupted nucleoli in *TifIa* single and *TifIa/Pten* double-knockout mice (arrows). Scale bars = 200 μm. *B*) Quantification of TH^+ cell numbers in *TifIa* and *TifIa/Pten* double-knockout mice 8 wk after the first Tam injection, normalized to the number of TH^+

(*continued on next page*)

intensive discussion (15, 44). Particularly attractive is the hypothesis that activation of the prosurvival Akt/mTOR pathway protects postmitotic neurons from endogenous and exogenous neurotoxic insults without promoting tumorigenesis (45). Indeed, an adenovirus-mediated overexpression of Akt in adult mouse DA neurons induces trophic effects and neuroprotection in the 6OHDA model of PD (46). Genetic deletion of *Pten* in developing DA neurons leads to similar neuroprotective effects accompanied by increases in total striatal dopamine content and in the number of TH^+ DA neurons in the ventral midbrain (22). However, in these genetic mutants, Pten expression is lost already at embryonic day 15 (E15; ref. 47), long before the onset of postnatal apoptotic death of DA neurons (48). Thus, the *Pten* deletion described by Diaz-Ruiz *et al.* (22) could affect postnatal development of the DA system and lead to the observed increase in TH^+ neuronal number because of the postnatal apoptosis inhibition. Therefore, the neuroprotective effects of Pten loss observed in the earlier study (22) could be due to the trophic effects of Akt/mTOR pathway activation during early postnatal development, and would not necessarily reflect the role of Pten in adult DA neurons.

The use of a BAC-based transgenesis with a temporally controlled Cre recombinase allows us to achieve a highly specific Pten ablation selectively in DA neurons in adult mice. Moreover, this inducible genetic system ensures higher targeting efficiency and specificity compared to virus-mediated transgene expression. In our study, *Pten* deletion led to activation of the Akt/mTOR pathway selectively in the adult DA neurons. While the number of TH^+ neurons in the substantia nigra and VTA regions was not affected, we observed the increased size of cell soma and nucleoli in this neuronal population, as well as more pronounced TH^+ neurofilaments in the substantia nigra reticulata and in the striatum.

The increase in striatal dopamine caused by *Pten* ablation did not lead to any behavioral changes in open field, wire hang, and grip strength tests and in the rotarod assay. These results are in line with recently reported data indicating that *Pten* deletion in DA neurons during embryonic development leads to the increase in striatal dopamine content, but does not change extracellular dopamine dynamics (22). Adult-onset ablation of *Pten* did not significantly affect the levels of PD-related protein PINK1 in the ventral midbrain of *Pten*-knockout mice. The absence of the behavioral phenotype after the adult DA-specific *Pten* deletion in our study also indicates that, in contrast to the brain-specific *Pten* deletion that causes defects in the synaptic structure and myelination abnormalities (18), the adult onset *Pten* ablation did not lead to any obvious deleterious functional changes, such as the loss of TH^+ neurons or reduced performance in a rotarod assay, even up to 35 wk after the deletion onset (data not shown).

Here, we demonstrate that *Pten* ablation resulted in the increased expression not only of *TH*, but also of *En1, Pitx3, Nurr1, Lmx1b,* and *Foxa2*. These genes play crucial roles in the development of midbrain DA neurons (36). During embryonic development, forkhead transcription factors Foxa1 and Foxa2 regulate the expression of Lmx1a and Lmx1b and are required for the expression of En1 and Nurr1 in immature DA neurons (35, 37). Foxa1 and Foxa2 cooperate with Pitx3 and Nurr1 to promote TH expression during late DA neuron differentiation (34, 37). The expression of these factors continues in the midbrain DA neurons through adulthood; moreover, haploinsufficiency for *Foxa2* or *En1/2*, or adult-onset deletion of *Nurr1* lead to a progressive loss of midbrain DA neurons and decline in striatal dopamine, resulting in the development of PD-like phenotype in adult mice (39, 49–51). Decreased *Nurr1* expression, as well as mutations and polymorphisms in this gene, have also been identified in some cases of early-onset PD (52–54). In combination with our results, these data support the hypothesis that the developmental Foxa1/2-regulated gene expression network is functional also in the adult animals, promoting the expression of TH. We demonstrate here that *Pten* ablation results in the up-regulation of *Foxa2,* as well as *En1, Pitx3, Lmx1b,* and *Nurr1* expression, leading to the increase in TH levels in the ventral midbrain and rising striatal dopamine content.

In this study, we show that the adult-onset *Pten* deletion is neuroprotective in a genetic progressive model of PD caused by selective ablation of Pol I-specific transcription initiation factor *TifIa* in adult DA neurons (12). Adult-onset *TifIa* deletion leads to inhibition of ribosomal RNA synthesis, nucleolar disruption, progressive loss of TH^+ nigral DA neurons, and decline in striatal dopamine. This neurodegenerative phenotype may partly be due to the down-regulation of Akt/mTOR pathway observed in *TifIa*-knockout animals (11, 12). Therefore, we studied whether *Pten* deletion that activates Akt/mTOR signaling could attenuate a neurodegenerative phenotype caused by *TifIa* ablation. Despite the fact that *Pten* deletion could prevent neither nucleolar disruption nor the loss of nigral TH^+ neurons in *TifIa/Pten* double-knockout animals, the loss of *Pten* significantly attenuated the decline in striatal dopamine in *TifIa/Pten* double-knockout

cells in control mice. *C*) *Pten* deletion attenuates the progressive decline in striatal dopamine, measured by HPLC, in *TifIa*- and *TifIa/Pten*-knockout mice 6, 8, and 21 wk after Tam injections. Groups with different superscript letters are statistically different ($P<0.05$; 2-way ANOVA with Bonferroni *post hoc* test). *D*) Balance and motor coordination of control, *Pten*, *TifIa*-knockout, and *TifIa/Pten* double-knockout mice, as measured by a constant speed rotarod assay at 15, 25, 35, and 44 rpm at indicated time points after the first Tam injection. Graphs show mean latency to fall for the two trials at each speed level. All data are expressed as means ± SE. $^*P < 0.05$, $^{**}P < 0.01$, $^{***}P < 0.001$ *vs.* control mice; $^{\#}P < 0.05$, $^{\#\#\#}P < 0.001$ *vs. TifIa/Pten* ko mice; Student's unpaired *t* test.

compared to *TifIa* single-knockout mice. The protection against progressive loss of striatal dopamine after the activation of Akt/mTOR pathway in *TifIa/Pten* double-knockout mice may, at least partly, be due to the Akt-mediated suppression of retrograde axonal degeneration (55).One of the earliest behavioral abnormalities that we detected in *TifIa*-knockout mice was the asymmetry in overlap between forepaw and hindpaw placement. Asymmetric onset is a clinical characteristic of patients with PD (40–42) that has also been described for some mouse models of PD (39). Notably, this gait abnormality was present only in *TifIa* single-knockout, but not in *TifIa/Pten* double-knockout mice, further demonstrating the protective role of *Pten* deletion in this mouse model.

The increased striatal dopamine levels in *TifIa/Pten* double-knockout mice were paralleled by the amelioration of locomotor deficits in rotarod assay. *TifIa*-knockout mice exhibited progressive difficulties in maintaining the balance on a rotarod beginning at 10 wk after *TifIa* deletion, whereas *Pten* ablation rescued this phenotype. Interestingly, the first behavioral symptoms of PD in humans are observed when the striatal dopamine levels fall below 20% of their normal level (56). Similarly, *TifIa*-knockout mice exhibited first signs of motor deficits in rotarod assay at 8–10 wk after *TifIa* ablation, when the striatal dopamine content reached a threshold level of 20–25% compared with control mice. In *TifIa/Pten* double-knockout animals, the decline in striatal dopamine is attenuated, and the progression on locomotor phenotype is prevented, or at least significantly delayed.

To further characterize the neuroprotective potential of *Pten* deletion, we used 6OHDA and MPTP models of PD. In both models, *Pten* ablation prevented the toxin-induced decline in striatal dopamine. Moreover, Pten deletion attenuated the loss of TH^+ neurons in the substantia nigra of 6OHDA-treated animals. Correspondingly, our behavioral analysis revealed the presence of early signs of a gait disturbance in the form of overlap asymmetry in MPTP-treated control, but not *Pten*-knockout mice.

In this study, we demonstrate the neuroprotective role of *Pten* deletion in the adult DA neurons. Previous reports demonstrated that activation of Akt/mTOR pathway induces protection against DA neuron loss and axonal degeneration due to inhibition of excessive autophagy and apoptosis in toxin-induced models of PD (46, 55), whereas the repression of Akt/mTOR signaling in DA neurons is associated with mitochondrial dysfunctions and increased oxidative stress (12, 57). However, it was also shown that systemic administration of an mTOR inhibitor, rapamycin, is protective in mouse and fly models of Huntington's disease, Alzheimer's disease, and PD due to its effects on 4E-BP activation or induction of autophagy (58–60). A common conclusion emerging from these studies is that, apparently, a protective role of Akt/mTOR pathway can be highly context dependent and that normal cellular functions require a correct balance between Akt/mTOR overstimulation and repression. While overstimulation of Akt/mTOR signaling may result in accumulation of toxic proteins and damaged mitochondria due to insufficient levels of autophagy, its repression leads to neuronal atrophy, axonal degeneration, and cell death (61, 62).

The protective effects of *Pten* deletion observed in our study may result not only from Akt/mTOR pathway activation, as Pten was shown to be involved in the maintenance of mitochondrial function, mitophagy, and regulation of mitochondria-dependent apoptosis by preventing cytochrome *c* release and caspase 3 activation during toxic insults (17, 45, 63).

Our study extends the understanding of the neuroprotective mechanisms induced by selective *Pten* ablation in adult DA neurons in genetic and toxin-induced models of PD. We also suggest a molecular sequence of events, in which the loss of Pten up-regulates several factors important for the maintenance of the DA neuronal population, notably *Foxa2*, *Pitx3*, and *Nurr1*, that promote TH expression in ventral midbrain, leading to an increase in striatal dopamine content. The selective ablation of *Pten* in adult DA neurons excludes possible developmental effects arising when *Pten* is deleted during embryonic development (18, 22). Therefore, in addition to its proposed use in the treatment of brain injury after ischemic stroke (45, 64), specific inhibition of Pten-dependent functions in adult DA neuronal population serves as an attractive therapeutic approach to the treatment of PD. FJ

The authors thank R. Hertel for HPLC-ED. This work was supported by the Deutsche Forschungsgemeinschaft, through Collaborative Research Centers SFB 488 and SFB 636; the Fonds der Chemischen Industrie; the European Union, through grant LSHM-CT-2005-018652 (CRESCENDO); the Bundesministerium für Bildung und Forschung, through NGFNplus grants FZK 01GS08153 and 01GS08142 and project 0313074C (HepatoSys); the Helmholtz Gemeinschaft Deutscher Forschungszentren, through Initiative CoReNe and Alliance HelMA; and the Deutsche Krebshilfe, through project 108567.

REFERENCES

1. Klein, C., and Lohmann-Hedrich, K. (2007) Impact of recent genetic findings in Parkinson's disease. *Curr. Opin. Neurol.* **20,** 453–464
2. Terzioglu, M., and Galter, D. (2008) Parkinson's disease: genetic versus toxin-induced rodent models. *FEBS J.* **275,** 1384–1391
3. Schober, A. (2004) Classic toxin-induced animal models of Parkinson's disease: 6-OHDA and MPTP. *Cell Tissue Res.* **318,** 215–224
4. Abou-Sleiman, P. M., Muqit, M. M., and Wood, N. W. (2006) Expanding insights of mitochondrial dysfunction in Parkinson's disease. *Nat. Rev. Neurosci.* **7,** 207–219
5. Narendra, D. P., Jin, S. M., Tanaka, A., Suen, D. F., Gautier, C. A., Shen, J., Cookson, M. R., and Youle, R. J. (2010) PINK1 is selectively stabilized on impaired mitochondria to activate Parkin. *PLoS Biol.* **8,** e1000298
6. Matsuda, N., Sato, S., Shiba, K., Okatsu, K., Saisho, K., Gautier, C. A., Sou, Y. S., Saiki, S., Kawajiri, S., Sato, F., Kimura, M., Komatsu, M., Hattori, N., and Tanaka, K. (2010) PINK1 stabilized by mitochondrial depolarization recruits Parkin to dam-

aged mitochondria and activates latent Parkin for mitophagy. *J. Cell Biol.* **189,** 211–221
7. Sha, D., Chin, L. S., and Li, L. (2010) Phosphorylation of parkin by Parkinson disease-linked kinase PINK1 activates parkin E3 ligase function and NF-κB signaling. *Hum. Mol. Genet.* **19,** 352–363
8. Geisler, S., Holmstrom, K. M., Skujat, D., Fiesel, F. C., Rothfuss, O. C., Kahle, P. J., and Springer, W. (2010) PINK1/Parkin-mediated mitophagy is dependent on VDAC1 and p62/SQSTM1. *Nat. Cell Biol.* **12,** 119–131
9. Ekstrand, M. I., and Galter, D. (2009) The MitoPark Mouse—an animal model of Parkinson's disease with impaired respiratory chain function in dopamine neurons. *Parkinsonism Relat. Disord.* **15**(Suppl. 3), S185–S188
10. Dawson, T. M., Ko, H. S., and Dawson, V. L. (2010) Genetic animal models of Parkinson's disease. *Neuron* **66,** 646–661
11. Parlato, R., Kreiner, G., Erdmann, G., Rieker, C., Stotz, S., Savenkova, E., Berger, S., Grummt, I., and Schutz, G. (2008) Activation of an endogenous suicide response after perturbation of rRNA synthesis leads to neurodegeneration in mice. *J. Neurosci.* **28,** 12759–12764
12. Rieker, C., Engblom, D., Kreiner, G., Domanskyi, A., Schober, A., Stotz, S., Neumann, M., Yuan, X., Grummt, I., Schutz, G., and Parlato, R. (2011) Nucleolar disruption in dopaminergic neurons leads to oxidative damage and parkinsonism through repression of mammalian target of rapamycin signaling. *J. Neurosci.* **31,** 453–460
13. Cully, M., You, H., Levine, A. J., and Mak, T. W. (2006) Beyond PTEN mutations: the PI3K pathway as an integrator of multiple inputs during tumorigenesis. *Nat. Rev. Cancer* **6,** 184–192
14. Zhang, C., Comai, L., and Johnson, D. L. (2005) PTEN represses RNA polymerase I transcription by disrupting the SL1 complex. *Mol. Cell. Biol.* **25,** 6899–6911
15. Kim, R. H., and Mak, T. W. (2006) Tumours and tremors: how PTEN regulation underlies both. *Br. J. Cancer* **94,** 620–624
16. Kim, R. H., Peters, M., Jang, Y., Shi, W., Pintilie, M., Fletcher, G. C., DeLuca, C., Liepa, J., Zhou, L., Snow, B., Binari, R. C., Manoukian, A. S., Bray, M. R., Liu, F. F., Tsao, M. S., and Mak, T. W. (2005) DJ-1, a novel regulator of the tumor suppressor PTEN. *Cancer Cell* **7,** 263–273
17. Zhu, Y., Hoell, P., Ahlemeyer, B., Sure, U., Bertalanffy, H., and Krieglstein, J. (2007) Implication of PTEN in production of reactive oxygen species and neuronal death in in vitro models of stroke and Parkinson's disease. *Neurochem. Int.* **50,** 507–516
18. Fraser, M. M., Bayazitov, I. T., Zakharenko, S. S., and Baker, S. J. (2008) Phosphatase and tensin homolog, deleted on chromosome 10 deficiency in brain causes defects in synaptic structure, transmission and plasticity, and myelination abnormalities. *Neuroscience* **151,** 476–488
19. Backman, S. A., Stambolic, V., Suzuki, A., Haight, J., Elia, A., Pretorius, J., Tsao, M. S., Shannon, P., Bolon, B., Ivy, G. O., and Mak, T. W. (2001) Deletion of Pten in mouse brain causes seizures, ataxia and defects in soma size resembling Lhermitte-Duclos disease. *Nat. Genet.* **29,** 396–403
20. Groszer, M., Erickson, R., Scripture-Adams, D. D., Lesche, R., Trumpp, A., Zack, J. A., Kornblum, H. I., Liu, X., and Wu, H. (2001) Negative regulation of neural stem/progenitor cell proliferation by the Pten tumor suppressor gene in vivo. *Science* **294,** 2186–2189
21. Van Diepen, M. T., and Eickholt, B. J. (2008) Function of PTEN during the formation and maintenance of neuronal circuits in the brain. *Dev. Neurosci.* **30,** 59–64
22. Diaz-Ruiz, O., Zapata, A., Shan, L., Zhang, Y., Tomac, A. C., Malik, N., de la Cruz, F., and Backman, C. M. (2009) Selective deletion of PTEN in dopamine neurons leads to trophic effects and adaptation of striatal medium spiny projecting neurons. *PLoS One* **4,** e7027
23. Lesche, R., Groszer, M., Gao, J., Wang, Y., Messing, A., Sun, H., Liu, X., and Wu, H. (2002) Cre/loxP-mediated inactivation of the murine Pten tumor suppressor gene. *Genesis* **32,** 148–149
24. Engblom, D., Bilbao, A., Sanchis-Segura, C., Dahan, L., Perreau-Lenz, S., Balland, B., Parkitna, J. R., Lujan, R., Halbout, B., Mameli, M., Parlato, R., Sprengel, R., Luscher, C., Schutz, G., and Spanagel, R. (2008) Glutamate receptors on dopamine neurons control the persistence of cocaine seeking. *Neuron* **59,** 497–508
25. Yuan, X., Zhou, Y., Casanova, E., Chai, M., Kiss, E., Grone, H. J., Schutz, G., and Grummt, I. (2005) Genetic inactivation of the transcription factor TIF-IA leads to nucleolar disruption, cell cycle arrest, and p53-mediated apoptosis. *Mol. Cell* **19,** 77–87
26. Zaborszky, L., and Vadasz, C. (2001) The midbrain dopaminergic system: anatomy and genetic variation in dopamine neuron number of inbred mouse strains. *Behav. Genet.* **31,** 47–59
27. Otto, D., and Unsicker, K. (1990) Basic FGF reverses chemical and morphological deficits in the nigrostriatal system of MPTP-treated mice. *J. Neurosci.* **10,** 1912–1921
28. Schober, A., Peterziel, H., von Bartheld, C. S., Simon, H., Krieglstein, K., and Unsicker, K. (2007) GDNF applied to the MPTP-lesioned nigrostriatal system requires TGF-β for its neuroprotective action. *Neurobiol. Dis.* **25,** 378–391
29. Carter, R. J., Lione, L. A., Humby, T., Mangiarini, L., Mahal, A., Bates, G. P., Dunnett, S. B., and Morton, A. J. (1999) Characterization of progressive motor deficits in mice transgenic for the human Huntington's disease mutation. *J. Neurosci.* **19,** 3248–3257
30. Carter, R. J., Morton, J., and Dunnett, S. B. (2001) Motor coordination and balance in rodents. *Curr. Protoc. Neurosci.* Chap. 8, Unit 8.12
31. Indra, A. K., Warot, X., Brocard, J., Bornert, J. M., Xiao, J. H., Chambon, P., and Metzger, D. (1999) Temporally-controlled site-specific mutagenesis in the basal layer of the epidermis: comparison of the recombinase activity of the tamoxifen-inducible Cre-ER(T) and Cre-ER(T2) recombinases. *Nucleic Acids Res.* **27,** 4324–4327
32. Parkitna, J. R., Engblom, D., and Schutz, G. (2009) Generation of Cre recombinase-expressing transgenic mice using bacterial artificial chromosomes. *Methods Mol. Biol.* **530,** 325–342
33. Unoki, M., and Nakamura, Y. (2001) Growth-suppressive effects of BPOZ and EGR2, two genes involved in the PTEN signaling pathway. *Oncogene* **20,** 4457–4465
34. Jacobs, F. M., van Erp, S., van der Linden, A. J., von Oerthel, L., Burbach, J. P., and Smidt, M. P. (2009) Pitx3 potentiates Nurr1 in dopamine neuron terminal differentiation through release of SMRT-mediated repression. *Development* **136,** 531–540
35. Ferri, A. L., Lin, W., Mavromatakis, Y. E., Wang, J. C., Sasaki, H., Whitsett, J. A., and Ang, S. L. (2007) Foxa1 and Foxa2 regulate multiple phases of midbrain dopaminergic neuron development in a dosage-dependent manner. *Development* **134,** 2761–2769
36. Smidt, M. P., and Burbach, J. P. (2007) How to make a mesodiencephalic dopaminergic neuron. *Nat. Rev. Neurosci.* **8,** 21–32
37. Lin, W., Metzakopian, E., Mavromatakis, Y. E., Gao, N., Balaskas, N., Sasaki, H., Briscoe, J., Whitsett, J. A., Goulding, M., Kaestner, K. H., and Ang, S. L. (2009) Foxa1 and Foxa2 function both upstream of and cooperatively with Lmx1a and Lmx1b in a feedforward loop promoting mesodiencephalic dopaminergic neuron development. *Dev. Biol.* **333,** 386–396
38. Brooks, S. P., and Dunnett, S. B. (2009) Tests to assess motor phenotype in mice: a user's guide. *Nat. Rev. Neurosci.* **10,** 519–529
39. Kittappa, R., Chang, W. W., Awatramani, R. B., and McKay, R. D. (2007) The foxa2 gene controls the birth and spontaneous degeneration of dopamine neurons in old age. *PLoS Biol.* **5,** e325
40. Lewek, M. D., Poole, R., Johnson, J., Halawa, O., and Huang, X. (2010) Arm swing magnitude and asymmetry during gait in the early stages of Parkinson's disease. *Gait Posture* **31,** 256–260
41. Yogev, G., Plotnik, M., Peretz, C., Giladi, N., and Hausdorff, J. M. (2007) Gait asymmetry in patients with Parkinson's disease and elderly fallers: when does the bilateral coordination of gait require attention? *Exp. Brain Res.* **177,** 336–346
42. Gelb, D. J., Oliver, E., and Gilman, S. (1999) Diagnostic criteria for Parkinson disease. *Arch. Neurol.* **56,** 33–39
43. Monville, C., Torres, E. M., and Dunnett, S. B. (2006) Comparison of incremental and accelerating protocols of the rotarod test for the assessment of motor deficits in the 6-OHDA model. *J. Neurosci. Methods* **158,** 219–223
44. Inzelberg, R., and Jankovic, J. (2007) Are Parkinson disease patients protected from some but not all cancers? *Neurology* **69,** 1542–1550

45. Chang, N., El-Hayek, Y. H., Gomez, E., and Wan, Q. (2007) Phosphatase PTEN in neuronal injury and brain disorders. *Trends Neurosci.* **30,** 581–586
46. Ries, V., Henchcliffe, C., Kareva, T., Rzhetskaya, M., Bland, R., During, M. J., Kholodilov, N., and Burke, R. E. (2006) Oncoprotein Akt/PKB induces trophic effects in murine models of Parkinson's disease. *Proc. Natl. Acad. Sci. U. S. A.* **103,** 18757–18762
47. Backman, C. M., Malik, N., Zhang, Y., Shan, L., Grinberg, A., Hoffer, B. J., Westphal, H., and Tomac, A. C. (2006) Characterization of a mouse strain expressing Cre recombinase from the 3′ untranslated region of the dopamine transporter locus. *Genesis* **44,** 383–390
48. Burke, R. E. (2004) Ontogenic cell death in the nigrostriatal system. *Cell Tissue Res.* **318,** 63–72
49. Sonnier, L., Le Pen, G., Hartmann, A., Bizot, J. C., Trovero, F., Krebs, M. O., and Prochiantz, A. (2007) Progressive loss of dopaminergic neurons in the ventral midbrain of adult mice heterozygote for Engrailed1. *J. Neurosci.* **27,** 1063–1071
50. Kadkhodaei, B., Ito, T., Joodmardi, E., Mattsson, B., Rouillard, C., Carta, M., Muramatsu, S., Sumi-Ichinose, C., Nomura, T., Metzger, D., Chambon, P., Lindqvist, E., Larsson, N. G., Olson, L., Bjorklund, A., Ichinose, H., and Perlmann, T. (2009) Nurr1 is required for maintenance of maturing and adult midbrain dopamine neurons. *J. Neurosci.* **29,** 15923–15932
51. Sgado, P., Alberi, L., Gherbassi, D., Galasso, S. L., Ramakers, G. M., Alavian, K. N., Smidt, M. P., Dyck, R. H., and Simon, H. H. (2006) Slow progressive degeneration of nigral dopaminergic neurons in postnatal Engrailed mutant mice. *Proc. Natl. Acad. Sci. U. S. A.* **103,** 15242–15247
52. Xu, P. Y., Liang, R., Jankovic, J., Hunter, C., Zeng, Y. X., Ashizawa, T., Lai, D., and Le, W. D. (2002) Association of homozygous 7048G7049 variant in the intron six of Nurr1 gene with Parkinson's disease. *Neurology* **58,** 881–884
53. Zheng, K., Heydari, B., and Simon, D. K. (2003) A common NURR1 polymorphism associated with Parkinson disease and diffuse Lewy body disease. *Arch. Neurol.* **60,** 722–725
54. Le, W., Pan, T., Huang, M., Xu, P., Xie, W., Zhu, W., Zhang, X., Deng, H., and Jankovic, J. (2008) Decreased NURR1 gene expression in patients with Parkinson's disease. *J. Neurol. Sci.* **273,** 29–33
55. Cheng, H. C., Kim, S. R., Oo, T. F., Kareva, T., Yarygina, O., Rzhetskaya, M., Wang, C., During, M., Talloczy, Z., Tanaka, K., Komatsu, M., Kobayashi, K., Okano, H., Kholodilov, N., and Burke, R. E. (2011) Akt suppresses retrograde degeneration of dopaminergic axons by inhibition of macroautophagy. *J. Neurosci.* **31,** 2125–2135
56. Fahn, S. (2003) Description of Parkinson's disease as a clinical syndrome. *Ann. N. Y. Acad. Sci.* **991,** 1–14
57. Malagelada, C., Ryu, E. J., Biswas, S. C., Jackson-Lewis, V., and Greene, L. A. (2006) RTP801 is elevated in Parkinson brain substantia nigral neurons and mediates death in cellular models of Parkinson's disease by a mechanism involving mammalian target of rapamycin inactivation. *J. Neurosci.* **26,** 9996–10005
58. Tain, L. S., Mortiboys, H., Tao, R. N., Ziviani, E., Bandmann, O., and Whitworth, A. J. (2009) Rapamycin activation of 4E-BP prevents parkinsonian dopaminergic neuron loss. *Nat. Neurosci.* **12,** 1129–1135
59. Ravikumar, B., Vacher, C., Berger, Z., Davies, J. E., Luo, S., Oroz, L. G., Scaravilli, F., Easton, D. F., Duden, R., O'Kane, C. J., and Rubinsztein, D. C. (2004) Inhibition of mTOR induces autophagy and reduces toxicity of polyglutamine expansions in fly and mouse models of Huntington disease. *Nat. Genet.* **36,** 585–595
60. Spilman, P., Podlutskaya, N., Hart, M. J., Debnath, J., Gorostiza, O., Bredesen, D., Richardson, A., Strong, R., and Galvan, V. (2010) Inhibition of mTOR by rapamycin abolishes cognitive deficits and reduces amyloid-beta levels in a mouse model of Alzheimer's disease. *PLoS One* **5,** e9979
61. Cherra, S. J., and Chu, C. T. (2008) Autophagy in neuroprotection and neurodegeneration: A question of balance. *Future Neurol.* **3,** 309–323
62. Levine, B., and Yuan, J. (2005) Autophagy in cell death: an innocent convict? *J. Clin. Invest.* **115,** 2679–2688
63. Zhu, Y., Hoell, P., Ahlemeyer, B., and Krieglstein, J. (2006) PTEN: a crucial mediator of mitochondria-dependent apoptosis. *Apoptosis* **11,** 197–207
64. Liu, B., Li, L., Zhang, Q., Chang, N., Wang, D., Shan, Y., Wang, H., Feng, H., Zhang, L., Brann, D. W., and Wan, Q. (2010) Preservation of GABAA receptor function by PTEN inhibition protects against neuronal death in ischemic stroke. *Stroke* **41,** 1018–1026

Received for publication January 25, 2011.
Accepted for publication May 5, 2011.